TECTONICS, VOL. 9, NO. 3, PAGES 409-422, JUNE 1990

KINEMATIC CONSTRAINTS ON DISTRIBUTED LITHOSPHERIC DEFORMATION IN THE EQUATORIAL INDIAN OCEAN FROM PRESENT MOTION BETWEEN THE AUSTRALIAN AND INDIAN PLATES

Richard G. Gordon

Department of Geological Sciences,
Northwestern University, Evanston, Illinois

Charles DeMets

Naval Research Laboratory, Washington, D. C.

Donald F. Argus

Department of Geological Sciences,
Northwestern University, Evanston, Illinois

Abstract. From an expanded, accurate, and up-to-date data set comprising 110 spreading rates, 46 transform azimuths, and 151 earthquake slip vectors from the Indian Ocean and Gulf of Aden, we determine a new rigid plate model describing the motion since 3 Ma between India and Australia. The Euler vector (ω=0.313°/m.y. about 5°S, 78°E) lies near the middle of the equatorial, diffuse plate boundary dividing the Indian from the Australian plate and predicts a rate of north-south shortening along 85°E of 4±3 mm/yr, only 30% as fast as predicted by our prior model. The new model also predicts north-south extension of 6±2 mm/yr (at 68°E) along the western segment of the diffuse plate boundary, where our prior model predicted north-south contraction. Using data only along the Carlsberg and Central Indian ridges and no other plate boundaries, we show that plate motion data cannot be fit by a single Euler vector. However, the data are well fit by two Euler vectors when an east-west striking India-Australia plate boundary is assumed to intersect the Central Indian Ridge near the equator. The best location along the Central Indian Ridge for this triple junction is 6°S–3°S, with 95% confidence limits of 9°S–4°N, just west of a region of intense seismicity. The sense of deformation, as recorded in earthquake focal mechanisms, reverse faults mapped with reflection seismic data, and undulations in basement topography, surface gravity, and the geoid, agrees well with the north-south extension predicted in the western part and the north-south shortening predicted in the eastern part of the India-Australia boundary. The predicted rate of north-south shortening between 79°E and 86°E is consistent with the rate of shortening inferred from observed faulting and folding; shortening taken up by faulting is ~6 to 100 times greater than that taken up by the spectacular basement folds. Little of the rapid north-south shortening predicted east of ~86°E is taken up by crustal thickening. Instead, lithosphere is transported northeastward toward the Sumatra trench through strike-slip faulting and possible clockwise rotation. The failure of the convergent segment of the diffuse plate boundary to form a subducting trench provides some new observations that must be satisfied by models for the initiation of subduction. A model of separate, rigid Indian and Australian plates divided by a diffuse plate boundary appears to be valid and useful because the predictions of the model agree with independent data and because the predicted velocity of relative motion is statistically significant and comparable with that across other plate boundaries.

Paper number 89TC03066.
0278-7407/90/89TC-03066$10.00

INTRODUCTION

The Indian Ocean basin presents a challenge to conventional plate tectonics because large earthquakes and deformation occur far from well-defined spreading centers, transform faults, and trenches (Figure 1). Large earthquakes have occurred along and near the Ninetyeast and Chagos-Laccadive ridges and in the Wharton and Central Indian basins [Gutenberg and Richter, 1954; Sykes, 1970; Stein and Okal, 1978; Stein, 1978; Wiens and Stein, 1983, 1984; Bergman et al., 1984; Bergman and Solomon, 1985; Wiens, 1986]. Focal mechanisms suggest left-lateral strike-slip motion along north-south striking fault planes within the active seismic zone (north of ~10°S) along the Ninetyeast ridge. Earthquakes within a few hundred kilometers east and west of the Ninetyeast ridge typically are strike-slip; earthquakes between 84°E and 86°E occur mainly on thrust

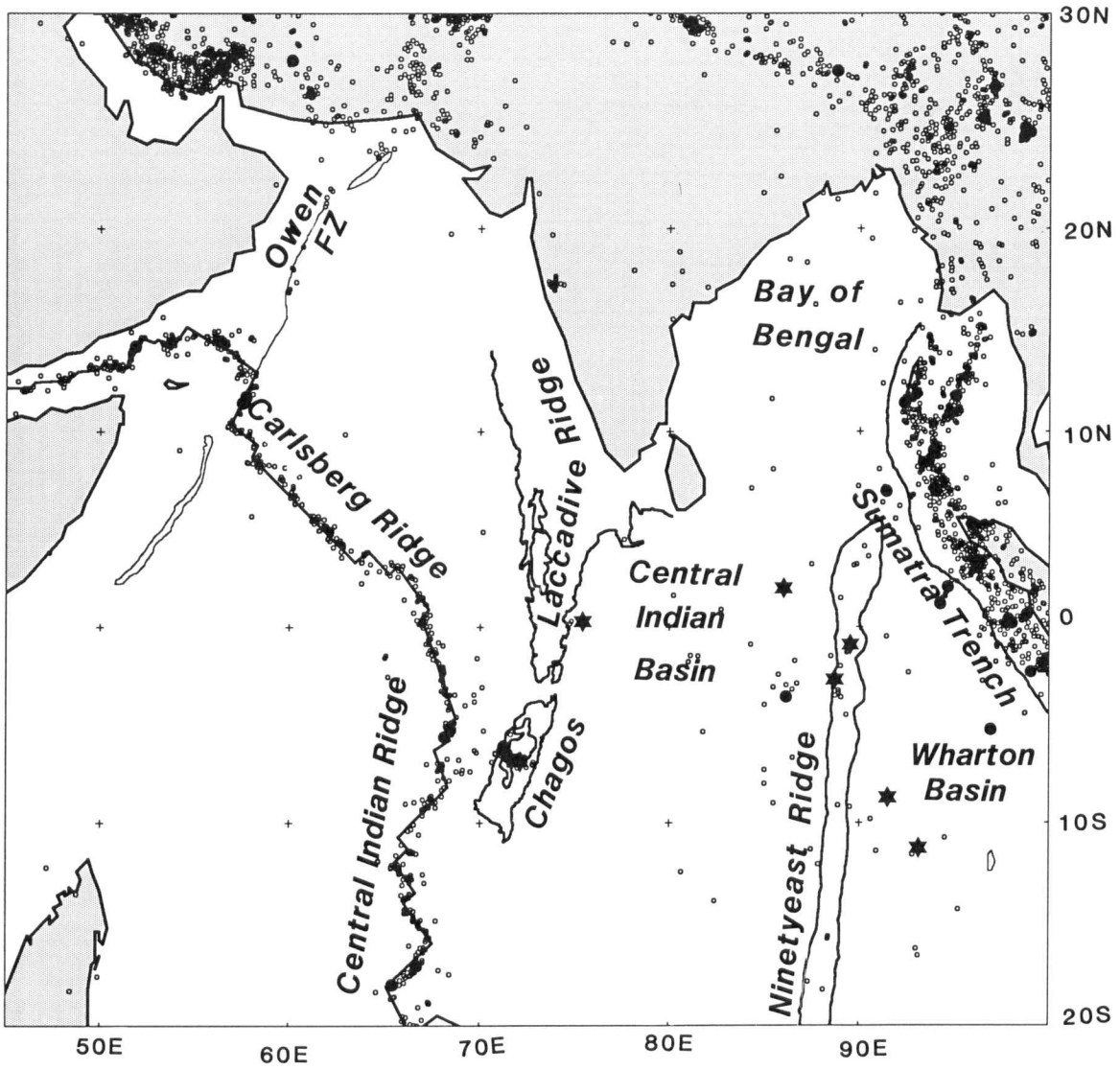

Fig. 1. Geography and seismicity of the central Indian Ocean. Shallow (less than 50 km deep) seismicity in the Indian Ocean region from 1963 through 1985 was taken from the Earthquake Data File of the National Geophysical Data Center. Locations of some large historic earthquakes [Petroy and Wiens, 1989] are also shown. Stars show earthquakes with M_S of 7.0 or greater, solid circles show earthquakes with M_S of 5.5 to 7.0, and small open circles show earthquakes with M_S less than 5.5. In the text we use the term "Chagos-Laccadive ridge" to refer to the long composite ridge on which the Chagos Archipelago and the Laccadive islands lie. "Chagos Bank" is a shallow, submerged, atoll-formed bank; its approximate location atop the Chagos-Laccadive Ridge is shown in Figure 5.

faults with nearly east-west striking fault planes, suggesting north-south shortening [Stein and Okal, 1978; Bergman and Solomon, 1985]. The earthquakes include the largest known oceanic "intraplate" earthquake, the 1928 M 7.7 Ninetyeast ridge event. Seismicity near Chagos Bank includes large earthquakes in 1912 (M_S=6.8), 1957, 1965, and 1983 (M_S=7.6) [Wiens and Stein, 1984] and is characterized by normal faulting earthquakes with tensional axes oriented approximately north-south (Figure 2) [Wiens, 1986]. Further evidence of widespread deformation of equatorial Indian Ocean lithosphere includes reverse faulting and east-west trending undulations of the basement observed on reflection seismic profiles [Eittreim and Ewing, 1972; Weissel et al., 1980; Geller et al., 1983], lineated gravity

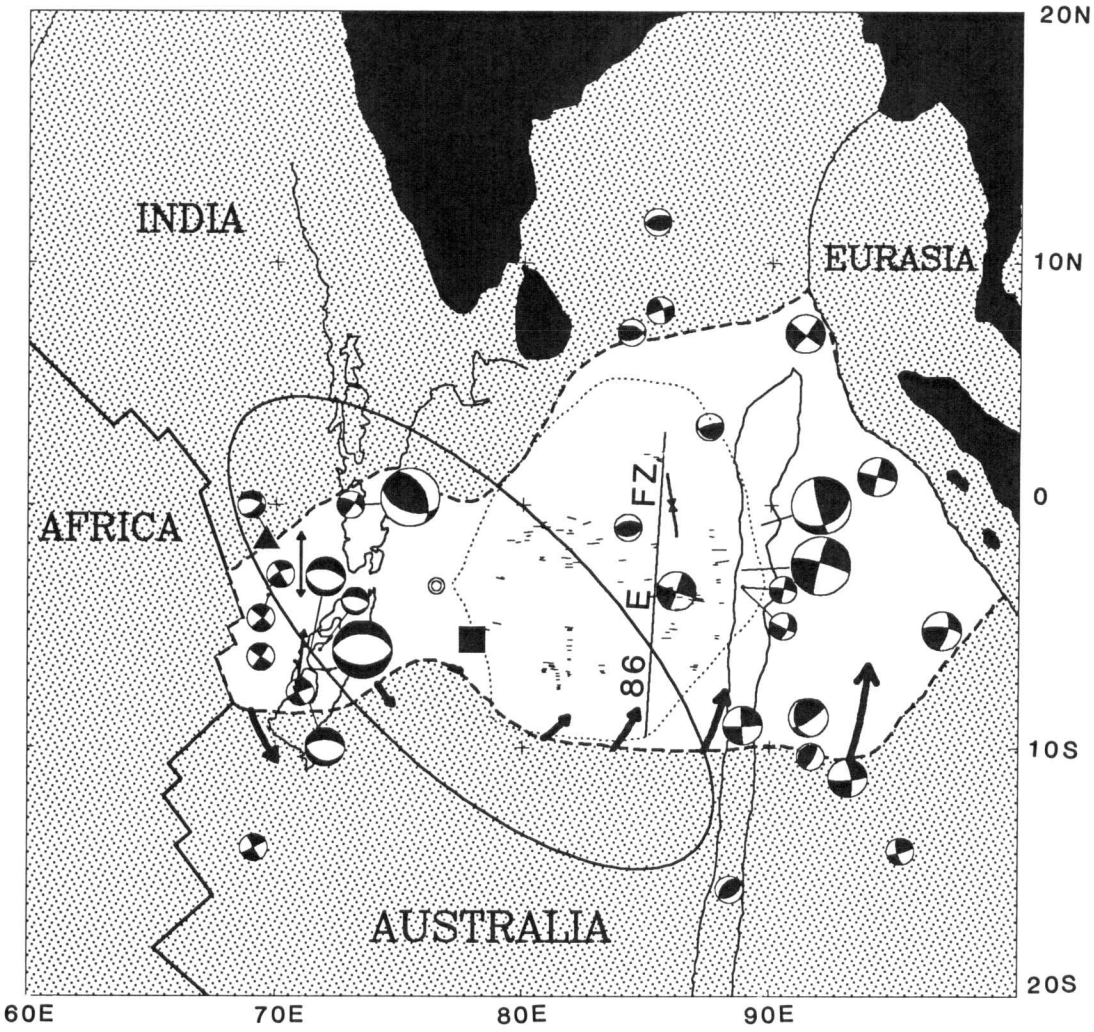

Fig. 2. Tectonic map and new model of central Indian Ocean deformation. A diffuse boundary (white area) divides the assumed-rigid Australian and Indian plates. The Australian plate moves counterclockwise relative to the Indian plate about an Euler pole (solid square), which has a 95% confidence region shown by the surrounding ellipse. The thick arrows on the Australian plate's northern border show the motion of the Australian plate relative to an arbitrarily fixed Indian plate. Thin lines within the diffuse boundary are faults with significant basement offsets. Dotted line shows approximate limits of area with east-west lineated gravity anomalies seen in Seasat data. Earthquake focal mechanisms and other deformation data suggest several distinct strain or stress provinces [cf., Zoback and Zoback, 1980] within the diffuse plate boundary. Focal mechanism size increases with magnitude. The largest mechanisms have M_S exceeding 7.0; the middle-sized mechanisms have M_S between 6.0 and 7.0; the smallest mechanisms have M_S less than 6.0. The two northernmost mechanisms with M_S exceeding 7.0 are historical mechanisms that are probably less well constrained than the other mechanisms shown. The mechanisms are taken from Stein [1978], Stein and Okal [1978], Dziewonski and Woodhouse [1983], Wiens and Stein [1984], Bergman et al. [1984], Bergman and Solomon [1985], Dziewonski et al. [1985], J. Woodhouse (personal communication, 1988), and Wiens [1986]. Thin arrows show two average tensional axes for nine focal mechanisms near the Central Indian Ridge and an average compressional axis for four mechanisms near the Ninetyeast ridge. The solid triangle is the Euler vector of Wiens et al. [1985], and the open circle is our Euler vector determined assuming India and Arabia lie on the same plate.

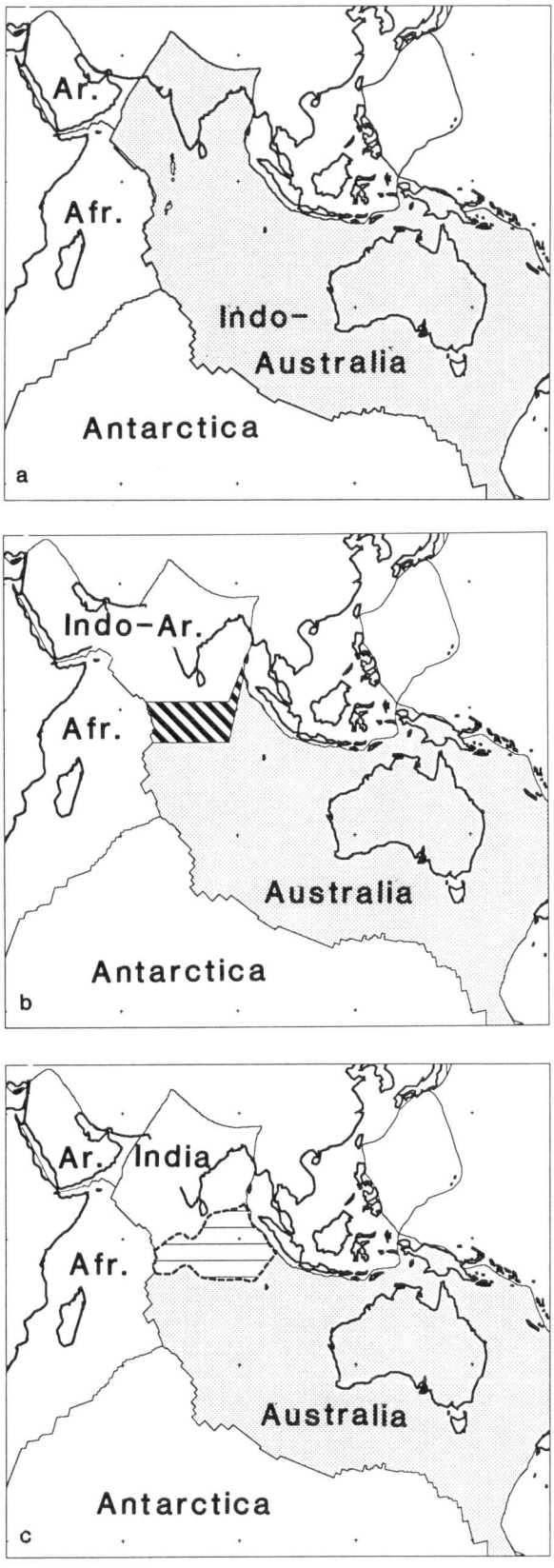

and geoid anomalies over the basement undulations [McAdoo and Sandwell, 1985; Zuber, 1987], and large heat flow anomalies [Geller et al., 1983]. The emerging picture of deformation is left-lateral strike-slip motion along planes subparallel to the Ninetyeast ridge, north-south contraction in the Central Indian Basin, and north-south extension near the Chagos-Laccadive Ridge.

Most workers have interpreted this well-documented zone of lithospheric deformation as part of a nonrigid Indo-Australian plate (Figure 3a). In a prior paper, however, we proposed an alternative rigid plate model: a diffuse plate boundary divides an Australian plate from an Indo-Arabian plate [Wiens et al., 1985]. The diffuse boundary trends east-west from the Central Indian Ridge near Chagos Bank to the Ninetyeast ridge and north along the Ninetyeast ridge to the Sumatra Trench (Figure 3b), thus including the regions of large earthquakes and basement faulting and folding. We previously showed that spreading rates and transform fault trends along the Carlsberg Ridge are fit significantly better by the new model (Figure 3b) than they are by the conventional plate model.

Here we improve our previously proposed plate motion model, compare predictions with independent observations, and consider some of the implications of the model. Unlike our prior study, we have modeled India and Arabia as distinct plates divided, in part, along the Owen fracture zone (Figure 3c) [Gordon and DeMets, 1989]. Motion along this boundary is slow and uncertain, and these uncertainties are incorporated into our error estimate for India-Australia motion. We also examine the sensitivity of the calculated location of the India-Australia Euler vector to the assumption we made before that Arabia is fixed relative to India. We examine the consistency of the predicted directions and rates of India-Australia deformation with independent observations and quantify the limits on the location of the intersection of the hypothesized diffuse plate boundary with the Central Indian Ridge.

We analyze all available Indian Ocean and Gulf of Aden plate motion data, ~4 times as many as used in our prior study. These data, which reflect some important revisions to spreading rates and transform-fault trends, are documented in detail elsewhere [DeMets et al., 1988; Gordon and DeMets, 1989], and we summarize them only briefly here.

Fig. 3. Proposed plate geometries for the Indian Ocean. (a) The conventional plate geometry. India and Australia lie on the same plate (the Indo-Australian plate). The Arabian plate is divided from the Indo-Australian plate along a boundary that includes the Owen fracture zone. (b) The geometry of Wiens et al. [1985]. Australia and India lie on separate plates (divided by a boundary that is mainly diffuse), and India and Arabia lie on the same plate (the Indo-Arabian plate). Motion along the Owen fracture zone is neglected. (c) The geometry that best describes current plate motions. Australia, India, and Arabia lie on distinct plates. The Australian and Indian plates are divided by a diffuse plate boundary, and the Arabian and Indian plates are divided by a boundary that includes the Owen fracture zone.

All spreading rates were determined by comparison of synthetic magnetic anomalies with observed profiles. We analyzed digital magnetic profiles obtained from the National Geophysical Data Center (NGDC) wherever available and analyzed enlarged versions of published figures for the minority of profiles unavailable from the NGDC. Transform fault azimuths were estimated mainly from published bathymetric data, supplemented by a few azimuths estimated from Seasat data. Earthquake slip vectors were determined almost entirely from published focal mechanisms, including many from the Harvard centroid-moment tensor solutions.

IS INDIA-AUSTRALIA MOTION MEASURABLE?

Prior studies found significant nonclosure of plate motion circuits in the Indian Ocean if the conventional plate geometry (Figure 3a) is assumed. Minster and Jordan [1978] and Stein and Gordon [1984] noted that the fit to Indian Ocean plate motion data could be improved if India and Australia are assumed to lie on separate plates divided along a hypothetical plate boundary following the Ninetyeast ridge [Stein and Okal, 1978] and continuing southward or southwestward to intersect the Southeast Indian Ridge. Wiens et al. [1985] showed that the inconsistencies in Indian Ocean plate circuits are lessened if India and Australia are assumed to be divided along a diffuse east-west trending plate boundary that intersects the equatorial Central Indian Ridge instead of the Southeast Indian Ridge. From spreading rates, transform azimuths, and earthquake slip vectors along the Southeast Indian Ridge, DeMets et al. [1988] furthermore showed that any boundary that follows the Ninetyeast ridge and intersects the Southeast Indian Ridge can take up no more than a few millimeters per year of motion. From these prior studies it was nevertheless unclear if the data require a triple junction along the Central Indian Ridge or if this was merely the most efficient location to add adjustable parameters to lessen the overall misfit within a complex system of plate circuits.

To eliminate these ambiguities, here we use data along only the Central Indian and Carlsberg ridges. If India and Australia were on the same plate, the Euler vector determined from plate motion data along only the Central Indian Ridge would predict rates and azimuths along the Carlsberg Ridge in agreement with observed rates and azimuths. However, no single Euler vector predicts motion consistent with data along both ridges. For example, the solid curve on Figure 4 shows the predictions from an Euler vector determined only from Central Indian Ridge plate motion data south of 5°S. The uncertainties in the rates predicted by this Euler vector along the Carlsberg Ridge are illustrated by 3 dashed vertical bars showing ±1-σ (i.e., standard) errors. The 95% confidence limits (±1.96-σ) of the predictions exclude the rates observed along the western Carlsberg Ridge.

The case for inconsistencies in transform fault azimuths is weaker. Although the strike of the well-surveyed Owen transform fault is 24° clockwise of the strike predicted by the Central Indian Ridge Euler vector, the 95% confidence limits of the prediction are large (±60°) and include the observed strike. Similarly, the 95% confidence limits of the transform azimuths along the southern Central Indian Ridge predicted by the Euler vector fit only to Carlsberg Ridge data (long-dashed curve in Figure 4) include the observed azimuths, although the ±1-σ limits shown in Figure 4 exclude the observed azimuths.

A stronger, more rigorous test of the consistency of the data with a fit to a single Euler vector is given by a statistical test for additional plate boundaries [Stein and Gordon, 1984]. As is described further below, this test shows that plate motion data along the Carlsberg Ridge cannot reflect motion between the same pair of plates as recorded along the Central Indian Ridge south of the equator. Thus we obtain an important new result: irrespective of data along other plate boundaries, data along the Central Indian and Carlsberg ridges cannot be fit by a single Euler vector. Therefore motion between India and Australia is measurable with plate motion data.

LOCATION OF THE INDIA-AUSTRALIA-AFRICA TRIPLE JUNCTION ALONG THE CARLSBERG OR CENTRAL INDIAN RIDGES

To quantify the best estimate and confidence limits of the location of the India-Australia-Africa triple junction determined from the plate motion data, we use methods proposed by Stein and Gordon [1984]. We consider many hypothetical locations along the Central Indian Ridge and Carlsberg Ridge for the location of the triple junction and determine the best fitting plate motion model for each. Our best estimate of the triple junction location is the estimate giving the model with the best fit to the data, as shown by the lowest value of

$$\chi^2 = \sum_{i=1}^{N} \left[\frac{d_i^{obs} - d_i^{pred}}{\sigma_i} \right]^2 \quad (1)$$

where d_i^{pred} is the value of the ith datum predicted from a particular plate motion model, d_i^{obs} is its observed value, and σ_i is the standard error assigned to this observed datum. Confidence limits are determined from a chi-square test.

The 68 Central Indian and Carlsberg ridge plate motion data are best fit if the India-Australia-Africa triple junction is located between 2.8°S and 5.5°S, an interval without magnetic profiles, mapped transform faults, or earthquake focal mechanisms (Figures 4 and 5). The best estimate of the triple junction location nearly coincides in latitude with the Chagos seismic zone (Figures 1, 2, and 5). To determine whether the additional plate boundary is significant, we use an F ratio test based on the parameter

$$F_{4,N-7} = \frac{\chi^2(3) - \chi^2(7)}{\chi^2(7) / (N-7)} \quad (2)$$

where $\chi^2(3)$ is the value of chi-square for the best fitting model with only three adjustable parameters (i.e., trying to fit all data along the Central Indian and Carlsberg ridges by a single Euler vector), $\chi^2(7)$ is the value of chi-square for the best fitting model with seven adjustable parameters (three for the India-Africa Euler vector, 3 for the Australia-

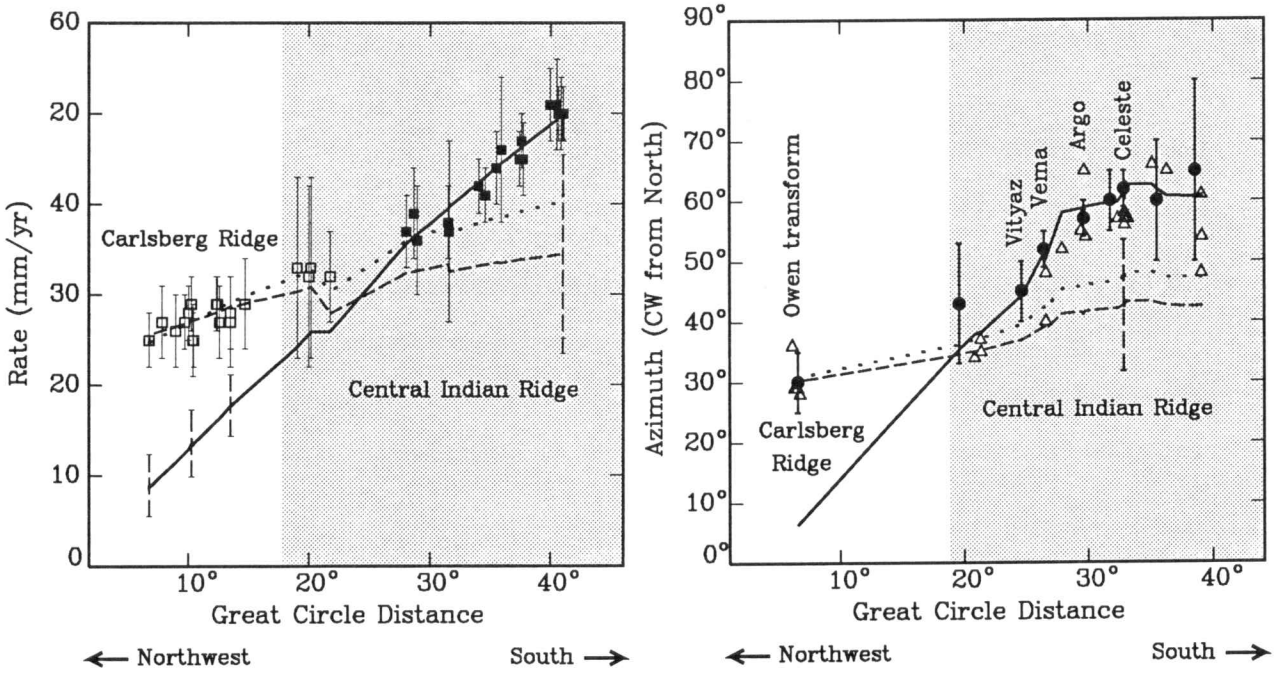

Fig. 4. Test of mutual consistency of plate motion data along the Central Indian and Carlsberg ridges. Data are compared with rates and azimuths calculated from different best fitting Euler vectors: best fitting vector (11.6°N, 50.8°E, 0.683°/m.y.) fit only to data south of 5°S along the Central Indian Ridge (solid curve), best fitting vector (28.3°N, 16.2°E, 0.338°/m.y.) fit only to data along the Carlsberg Ridge (long-dashed curve), and best fitting vector (25.5°N, 26.8°E, 0.409°/m.y.) fit to all data along the Carlsberg Ridge and to data north of 3°S along the Central Indian Ridge (short-dashed curve). Dashed vertical bars show plus and minus one standard error in predicted rates and azimuths at selected locations. Distance along the horizontal axis in each plot is proportional to the great circle distance of data locations from the Australia-Africa best fitting Euler vector. Squares show seafloor spreading rates determined from magnetic profiles, circles show observed transform fault azimuths, and triangles show observed slip vector azimuths. Data in the shaded region are located along the Central Indian Ridge; data in the unshaded region are located along the Carlsberg Ridge. The Australia-Africa Euler vector predicts rates along the Carlsberg Ridge that are significantly (9–20 mm/yr) slower than observed. Solid squares are rates we interpret in this paper as probably recording Australia-Africa motion; open squares are rates we interpret as probably recording India-Africa motion.

Africa Euler vector, and 1 for the latitude of the India-Australia-Africa triple junction), and N is the number of data. This statistic should be approximately F distributed with 4 versus N–7 degrees of freedom. The experimentally determined value of F can be compared with a reference value from tables [e.g., Spiegel, 1975] of $F_{4,N-7}$ with less than a 1% probability of being exceeded by chance.

We found that F equals 44.0, much larger than the reference value 3.6 for the 1% risk level; it is unlikely that the improvement in fit occurred by chance. The data do not preclude either a diffuse or a discrete India-Australia boundary where it intersects the Central Indian Ridge. The data are sparse between 12°S and 2°N, and the 95% confidence limits on the triple junction location range from 14°S to 5°N if data only along the Carlsberg and Central Indian ridges are used. If all data describing the relative motions of the African, Arabian, Indian, Australian, and Antarctic plates are used [DeMets et al., 1988; Gordon and DeMets, 1989], we find narrower confidence limits of 9°S to 4°N (Figure 5), an interval that is large but still encouragingly close to the Chagos seismic zone. The limited distance along the Central Indian Ridge where India-Africa and Australia-Africa rates are predicted to be similar (Figure 4) suggests that additional magnetic profiles could greatly narrow the limits on the location of the triple junction.

Although plate motion data limit the location of the western part of the boundary zone, they do not limit the zone eastward. The limits of the zone east of 78°E and near Chagos Bank are roughly defined by the limits of folds, faults, and locations of large earthquakes, but little faulting or folding occurs from 73°E to 78°E, where the Euler vector predicts no more than 1 mm/yr motion. Thus any structures

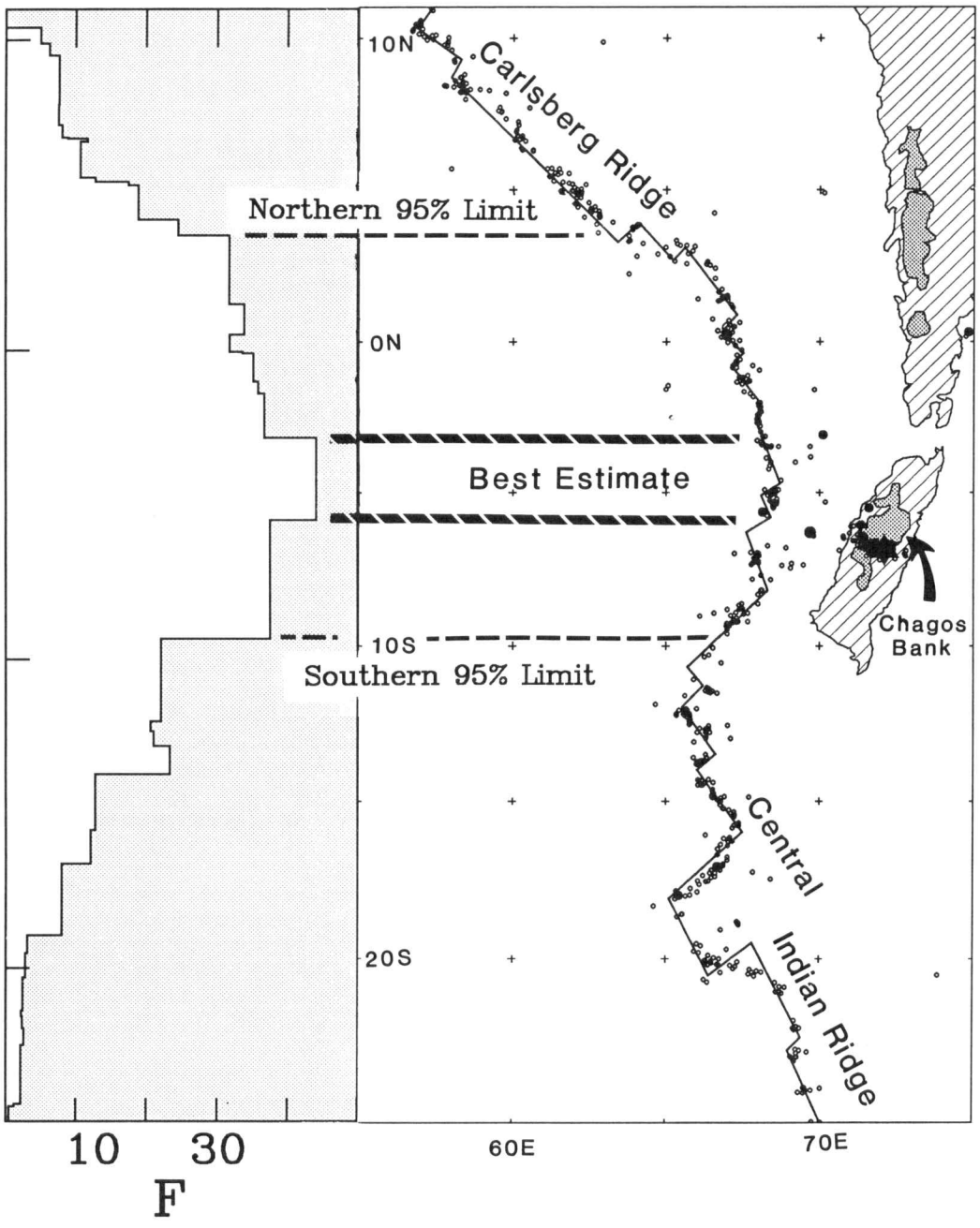

Fig. 5. Statistical limits on the location of the intersection of the India-Australia boundary with the Carlsberg and Central Indian ridges. The fit to the Central Indian Ridge and Carlsberg Ridge data of a single Euler vector is compared with the fit of two Euler vectors for many possible locations of a possible India-Africa-Australia triple junction. The data are best fit at the latitude giving the lowest value of χ^2, equivalent to the largest value of F, which is determined using formulas given by Stein and Gordon [1984] and is shown as a function of hypothetical boundary latitude. The best fit occurs anywhere between 2.8°S and 5.5°S, and the 95% confidence limits on the boundary location extend from 3.7°N to 9.3°S. The star marks the location of the November 30, 1983, $M_S = 7.6$ Chagos Bank earthquake.

that could help locate the boundary are probably poorly developed or nonexistent. The approximate edges of the boundary zone shown in Figure 2 exclude some magnitude 5 and smaller earthquakes lacking corroborating evidence for significant deformation.

INDIA-AUSTRALIA MOTION: MODEL AND COMPARISONS

India-Australia Motion Model

Because we use no data that directly reflect motion between India and Australia, our estimate is really the difference between Euler vectors describing India-Africa and Australia-Africa motion. To describe India-Africa motion as accurately as possible, we also used India-Arabia azimuths and Arabia-Africa plate motion data and required closure of the India-Arabia-Africa plate motion circuit. We have previously shown that the data describing the motion between the Indian, Arabian, and African plates are mutually consistent [Gordon and DeMets, 1989]. To describe Australia-Africa motion as accurately as possible we also used Africa-Antarctica and Australia-Antarctica plate motion data and required closure of the Australia-Antarctica-Africa plate motion circuit. We have also previously shown that the data describing motion between the Australian, Antarctic, and African plates are mutually consistent [DeMets et al., 1988].

The India-Australia Euler vector and confidence limits (Table 1) describe a model that differs from our prior model [Wiens et al., 1985] in several ways. The new India-Australia Euler vector lies 8° east and 4° south of the old Euler vector, predicting extension along a much longer segment of the India-Australia plate boundary (Figure 2). The 4±3 mm/yr rate of contraction predicted between a point (10°S, 85°E) on the Australian plate and a point (7°N, 85°E) on the Indian plate is only 30% as fast as the 14 mm/yr rate predicted by the old model. To test whether the differences between old and new Euler vectors are caused by the revised data or by the revised plate geometry (Figure 3c), we also determined an Euler vector for the motion of Australia relative to Indo-Arabia from our new data by deleting the plate motion data along the India-Arabia boundary and assuming that India and Arabia lie on the same plate. The resulting Euler vector (2.8°S, 75.8°E, 0.379°/m.y.) differs little from the new Australia-India Euler vector but predicts shortening rates that are 2–3 mm/yr faster. Thus the Euler vector depends only weakly on whether we treat India and Arabia as one or two plates, and most of the difference between the old and new Euler vectors is caused by the differences between the old and new data.

Comparison of Predicted Motion with Observed Orientations of Deformation

Many data not used to obtain our plate motion model record deformation in the diffuse boundary between India and Australia. These data place some limits on the sense and orientation of principal strains in the zone between the assumed rigid Indian and Australian plates. The simplest predictions made by our model are that east of the Euler vector the rigid Indian and Australian plates converge, while west of the Euler vector they diverge (Figure 2, Table 2).

Along a discrete plate boundary of known location and strike, the fault plane can in most cases be distinguished from the auxiliary nodal plane of focal mechanisms because the strike of one plane will parallel the strike of the boundary. Moreover, slip vectors from earthquakes along these discrete faults or plate boundaries will show a consistent direction of slip irrespective of whether they reflect strike-slip, dip-slip, or composite mechanisms of faulting. Regions of distributed deformation are less simple, however. One often cannot distinguish which nodal plane is the fault plane. Slip vectors typically show little consistency in direction. More often in these regions the principal stress axes inferred from the focal mechanisms show a consistent pattern [e.g., Zoback and Zoback, 1980], which might be related to the motion of the rigid plates that border the deforming region.

Three such consistent patterns have been observed in the Indian Ocean. One pattern is defined by earthquakes east of 86°E from 10°S to 10°N, which typically have strike-slip mechanisms but also include a few small events with reverse or thrust mechanisms (Figure 2). The strike-slip

TABLE 1. 0–3 Ma Euler Vectors Used in this Study

Plate Pair	Euler Vector			Standard Error Ellipse			
	°N	°E	ω, deg/m.y.	Semimajor Axis	Semiminor Axis	Azimuth of Major Axis	σ_ω, deg/m.y.
Australia-India	–5.5	77.7	0.31	7.5°	3.1°	N45°W	0.07
Australia-Africa	12.5	50.0	0.66	1.4°	0.9°	N35°W	0.01
Australia-Antarctica	13.1	37.6	0.68	1.3°	1.1°	N67°W	0.01
Africa-Antarctica	4.9	–38.4	0.14	6.0°	1.4°	N45°W	0.01
India-Africa	23.6	28.5	0.43	8.8°	1.5°	N74°W	0.06
India-Arabia	3.1	91.5	0.03	26.0°	2.4°	N58°W	0.04
Arabia-Africa	24.1	24.0	0.42	4.9°	1.3°	N65°W	0.05

First plate moves counterclockwise relative to second plate. Euler vectors were calculated for the present paper from the data of DeMets et al. [1988] and Gordon and DeMets [1989]. The Australia-Antarctica, Africa-Antarctica, and Australia-Africa Euler vectors differ slightly from and supersede those given by DeMets et al. [1988], which were erroneously calculated from data differing slightly from their final data set. σ_ω is the standard error of the rate of rotation.

TABLE 2. Predicted Rates of Change of Distance Between Points on the Indian and Australian Plates

Points on	Points on Australian Plate						
Indian Plate	10°S, 70°E	10°S, 75°E	10°S, 80°E	10°S, 85°E	10°S, 90°E	10°S, 95°E	10°S, 99°E
0.0°N, 70.0°E	5±2	3±1	1±1	0±1	−1±2	−1±2	−2±2
3.0°N, 75.0°E	3±2	2±2	0±2	−2±2	−3±1	−3±1	−4±1
3.0°N, 80.0°E	2±3	0±3	−1±3	−3±2	−4±2	−5±2	−5±1
7.0°N, 85.0°E	2±3	0±3	−2±3	−4±3	−6±3	−8±3	−8±3
8.0°N, 90.0°E	1±3	0±3	−2±4	−5±4	−7±4	−9±4	−10±3

Each rate is in millimeters per year and each uncertainty is ±1-σ. The distance between the points is predicted to increase if the rate of change is positive and to decrease if negative.

events have been interpreted as left-lateral faulting along approximately north-south fault planes (Figure 2) [Stein and Okal, 1978; Bergman and Solomon, 1985]. A second pattern is defined by thrust faulting earthquakes that are located in or near the southern Bay of Bengal and west of 86°E and which have compressional axes oriented approximately north-south (Figure 2) [Bergman and Solomon, 1985]. A third pattern is defined by normal-faulting earthquakes near Chagos Bank with tensional axes oriented approximately north-south. Several strike-slip earthquakes are located west of Chagos Bank, possibly on Central Indian Ridge fracture zones. The approximately north-south tensional axes of these events are consistent with extension of lithosphere west of and near the Chagos Bank (Figure 2) [Wiens, 1986].

Differing from these three patterns are focal mechanisms from two earthquakes located near 0°N, 73–75°E. These two earthquakes have approximately north-south compressional axes but occurred far west of other events with mechanisms indicating north-south compression. Unlike the other data they cannot be simply explained by the predictions of our Euler vector. Possibly these data indicate that our Euler vector is inaccurate or our model is wrong. However, these events may reflect stresses other than those caused by motion between India and Australia, or these mechanisms may be unreliable: one earthquake is small (M_0=7×10^{23} dyne cm) and the other is from historic (1944) data [Wiens, 1986]. Thus we ignore these events in our discussion below but recognize they may record motion more complex than our simple interpretation.

Data from 14 stress axes derived from focal mechanisms located within the diffuse boundary are summarized in Figure 2. The easternmost pair of arrows (located near the 86°E fracture zone), which average the compressional axes of five nearby events, is oriented N11°±10°W. The pair of arrows near 3°S, 71°E, which average the tensional axes of the three northern events, is oriented due north ±15°. The pair of arrows near 7°S, 71°E, which averages the tensional axes of six events near Chagos Bank, is oriented N07°±11°E.

Orientation of folds and faults east of 77°E can also be compared with the directions of shortening predicted by our plate motion model. Lithospheric deformation is reflected by large-scale folding of basement and by undulations in the geoid estimated from Geos 3 and Seasat altimetric data [Weissel et al., 1980; McAdoo and Sandwell, 1985]. The folds, which affect lithosphere from 9°S to 6°N between 78°E and 90°E, have axes striking ENE-WSW near the Ninetyeast ridge, and E-W to WNW-ESE near the southwestern Bengal Fan (~2°S, 83°E) [Weissel et al., 1980]. The approximately E-W to WSW-ENE orientation of the large-scale fold axes is nearly orthogonal to the N-NNW shortening direction predicted by the Australia-India Euler vector, agreeing reasonably with the predictions. Similarly, lineated gravity anomalies in the Wharton basin strike NE-SW [Haxby, 1987; Petroy and Wiens, 1989; Stein et al., 1989] and may be analogous to those in the Central Indian Basin. If so, they suggest a NW-SE direction of shortening, consistent with the sense of shortening predicted by our Euler vector.

Faults offsetting basement also record a component of motion. Marine seismic reflection profiles show increasing vertical offset of progressively older sediments along reverse faults, suggesting they are active [Weissel et al., 1980; Cochran et al., 1987]. The reverse faults strike east-west, consistent with a north-south component of shortening. Unfortunately the amount of strike-slip faulting is unknown.

In sum, the predictions of the relative motions of the rigid plates north and south of the diffuse plate boundary are consistent in sense with the north-south extension observed in the western part of the diffuse boundary and with the north-south to northwest-southeast contraction observed in the east part of the diffuse boundary.

Comparison of Predicted Motion with Observed Rates of Deformation

The precise rate of deformation within the boundary is hard to estimate independently of the plate motion model. A rate near the Ninetyeast ridge can be estimated from the historic seismic moment release in the region. This rate is a minimum rate for two reasons: (1) some slip may be aseismic, and (2) we interpret the Ninetyeast ridge seismic zone not as the entire plate boundary but as only part of a diffuse boundary. Stein and Okal [1978] estimated a seismic slip rate of ~20 mm/yr near the Ninetyeast ridge, but Petroy and Wiens [1989] estimated a slip rate of only ~3 mm/yr after redetermining the moments of large, pre-World-Wide Standard Seismograph Network events. The revised seismic slip rate is consistent with the predicted rate of shortening of 7±4 mm/yr between 10°S, 90°E and 8°N, 90°E (Table 2).

West of the 86°E fracture zone, in the area where only thrust earthquakes has been observed, the shortening rate in the folded and faulted region can be estimated using fold amplitudes and wavelengths and fault offsets. The horizon-

tal shortening taken up by folding can be estimated from the integral for the length of a sinusoidal plane curve [Thomas, 1972]:

$$\text{Restored length} = \int_0^L [1 + A^2k^2\cos^2(kx)]^{1/2}\, dx \qquad (3)$$

$$\approx L + A^2k^2L/4$$

where L is the length of the fold train, A is the fold amplitude, $k = 2\pi/\lambda$, and λ is the fold wavelength. The shortening is more sensitive to the fold amplitudes and wavelengths than to the north-south extent of the deformation zone. The large-scale folds of the lithosphere have characteristic wavelengths of 130 to 250 km and 1- to 3-km peak-to-trough amplitudes [Weissel et al., 1980; McAdoo and Sandwell, 1985]. Seismic reflection profiles show folded sediments and faults offsetting basement with vertical throws of up to 500 m [Weissel et al., 1980]. From equation (3), the total fold-related shortening is only 0.3 km using values of 190 km for the wavelength, a 1-km average amplitude [McAdoo and Sandwell, 1985], and an 1100-km fold train, estimated from the extent of the geoid undulations. Varying the fold amplitudes from 0.5 to 1.5 km, and the wavelengths from 130 to 250 km, the estimated shortening varies from 0.1 to 1.5 km.

Horizontal shortening also occurs by reverse faulting [Weissel et al., 1980; Geller et al., 1983]. Assuming that the steeply dipping fault surfaces observed in sediments and offsetting shallow basement rocks are planar, Geller et al. [1983] estimated the north-south contractional strain to be about 1%. If the shortening is homogeneous and occurs across an 1100 km north-south portion of the deforming zone, it would amount to 11 km. Thus any shortening caused by the long-wavelength folding of basement rocks is much smaller than the fault-related shortening. Unobserved shortening may also occur through pervasive crustal and lithospheric thickening. Geller et al. [1983] note that a 1% shortening should produce a heat flow anomaly of only 1 mW/m^2, far short of the observed heat flow anomalies of 10–40 mW/m^2. They suggest that a shortening of 4.5%, which would produce a heat flow anomaly of 20 mW/m^2, might be within the confidence limits of the amount of shortening they estimate from observed faulting. A 4.5% shortening over 1100 km gives an integrated shortening of 50 km.

Our model predicts that near 85°E the Australian plate has been approaching the Indian plate at 4±3 mm/yr for the past 3 m.y. (Table 2). Over 3 m.y. therefore, 12±9 km of shortening had to be taken up between India and Australia at this longitude. It would be a considerable coincidence if Geller et al.'s [1983] estimate of shortening did not reflect shortening over an interval longer than the 3 m.y. described by our model. The onset of central Indian Ocean deformation has been dated by a widespread 7 Ma unconformity in Bengal Fan sediments [Cochran et al., 1987]. Thus the shortening observed in the reverse faults may have accumulated over an interval more than twice as long as that covered by our plate motion model. If we assume that shortening has occurred at a constant rate over 7 m.y., our plate motion model would predict a total shortening of 28±21 km, consistent within its uncertainties with the values estimated from observed faulting and from observed heat flow [Geller et al., 1983].

To test our model further, we crudely estimated the extension rate near Chagos Bank as follows. From the seismic moment of the November 30, 1983, M_S 7.6 Chagos Bank earthquake, which gives most of the seismic moment release since the prior major earthquake in 1912, Schlanger and Stein [1987] estimate several meters of vertical seafloor motion. Because the earthquake focal mechanism shows slip along a plane dipping ~45°, the horizontal motion must also be several meters. If we assume that the recurrence interval between major earthquakes is ~70 years, the interval between the major 1912 and 1983 earthquakes, the slip rate is several millimeters per year, which is consistent with the 4±2 mm/yr rate of north-south extension predicted by our model.

The decrease in fold amplitude west of 80°E and decrease of folds, faults, and seismicity west of 78°E are also consistent with the predictions (Figure 2) because our Australia-India Euler vector, located at 78°E, predicts motion of less than 1 mm/yr for all points within 2° of it. The slow predicted motion from ~76°E to ~80°E is also consistent with the absence of seismicity between 74°E and 80°E.

DISCUSSION

Accommodation of North-South Shortening and Nature of Plate Boundary Zone East of 86°E

In our prior model [Wiens et al., 1985] we interpreted the Ninetyeast ridge seismic zone as a narrow boundary separating the Australian plate on the east from the Indian plate or part of the diffuse boundary on the west (Figure 3b). Following Stein and Okal [1978], we assumed that the large earthquakes rupture the major fracture zone lying just east of the Ninetyeast ridge. This interpretation is now untenable for several reasons. Significant strike-slip earthquakes occur up to ~1000 km east and several hundred kilometers west of the Ninetyeast Ridge (Figure 2). Recent estimates of the locations of large historical earthquakes near Ninetyeast ridge show that they do not occur on this fracture zone. Instead they occur along the Ninetyeast ridge, west of the ridge, and along the 86°E fracture zone [Petroy and Wiens, 1989]. East-west striking gravity anomalies thought to reflect north-south shortening in the Central Indian Basin may change strike to NE-SW and continue into the Wharton Basin [Haxby, 1987; Petroy and Wiens, 1989; Stein et al., 1989].

A wide-boundary model introduces kinematical complexities unneeded in our prior model in which all motion between Australia and India was transformed onto the discrete fault along the Ninetyeast Ridge, which in turn disappeared into the Sumatra trench (Figure 3b). The N-S to NW-SE contraction between 78°E and 86°E appears to be taken up by thickening of the crust and lithosphere through folding, near-surface reverse faulting, and deeper thrust faulting. East of 86°E, however, the data suggest little crustal and lithospheric thickening. Most earthquakes east of

86° have strike-slip focal mechanisms. The amplitudes of long-wavelength topographic and gravity anomalies diminish eastward across the 86°E fracture zone, as does the deformation of fan sediments [Geller et al., 1983]. Nevertheless, the rate of shortening across the boundary zone is predicted by the Euler vector to increase eastward.

If thickening is negligible, all the strike-slip is along north-south striking fault planes, and the motion is limited to north-south translations, no north-south shortening could occur. If the faults and intervening blocks in the deforming zone rotate clockwise, however, material could be transported eastward thereby accommodating north-south shortening. This explanation would require left-lateral strike-slip faulting along an east-west to northeast-southwest striking fault or faults near the contact between the Indian plate and the northern edge of the boundary zone. One small earthquake near 8°N, 85°E appears to have a mechanism permitting left-lateral slip along a ENE-WSW fault plane, possibly consistent with this model. Moreover, the event near 7°N, 91°E could accommodate left-lateral slip on a NE-striking fault plane, which may also be consistent with this model (Figure 2).

Alternatively, some of the strike-slip earthquakes within the deforming region may occur on east-west striking fault planes, permitting eastward transport of material. In this model the boundary zone deforms in pure shear with maximum extension in a southwest-northeast direction. Weighing against this suggestion is that no east-west striking structures that would provide a vertical fault plane are known, although many dipping faults that strike east-west have been recognized. The hypothesis of east-west fault planes in the strike-slip earthquakes could be tested by marine geophysical surveying of the seafloor structures or by mapping out earthquake aftershock distributions with an array of ocean bottom seismometers.

In both the models we suggest, convergence is accommodated through northeastward motion of material within the boundary zone, similar to the way in which north-south shortening has been proposed to be taken up in the collision between India and Eurasia where a major fraction of the convergence is taken up by lateral motion along strike-slip faults of the material between the converging blocks [Molnar and Tapponnier, 1975]. Presumably, the northeast transport of lithosphere within the India-Australia diffuse plate boundary is accommodated by increased lithospheric consumption in the Sumatra trench.

Nonsubducting Convergent Plate Boundary

The failure of the convergent segment of the India-Australia plate boundary to form a trench subducting oceanic lithosphere brings some new constraints to the problem of how subducting trenches form. McKenzie [1977] proposed two necessary conditions for trenches to form: First, the compressive stress must be high enough, about 80 MPa (800 bars), to overcome frictional resistance on a thrust fault through the entire mechanical lithosphere. Second, the downgoing plate must be underthrust fast enough that it does not warm too much to be negatively buoyant. McKenzie [1977] estimated the critical speed to be about 13 mm/yr, but this estimate is tenuous because it is inversely proportional to an estimate of the poorly known thermal time constant of subducting lithosphere. Neither of these conditions is easily satisfied in the Indian Ocean or elsewhere.

Because some recent estimates of the level of compressive stress in Indian Ocean lithosphere greatly exceed the minimum required by McKenzie's model, enough force may be available to start subduction, however. From a finite element model that includes the age dependence of slab pull and ridge push forces, Cloetingh and Wortel [1985] estimated the level of compressive stress to be several hundred megapascals. From their model for the buckling of Indian Ocean lithosphere, McAdoo and Sandwell [1985] estimate the average compressive stress to be about 600 MPa. These estimates are model dependent, however, and the real level of stress may be lower.

In any event, because the shortening in the diffuse plate boundary is taken up over a wide zone, the conditions for a trench to form may be even harder to satisfy than previously thought. The Indian Ocean diffuse plate boundary probably differs from the conditions considered by McKenzie [1977] because no evidence suggests that a thrust fault cuts the entire mechanical lithosphere. Where the rate of shortening is greatest, contraction appears to be taken up not by thrust faulting but by northeastward transport of lithosphere along strike-slip faults. Within the zone where thrust or reverse faulting is significant the nodal planes of the observed thrust-faulting earthquakes typically dip moderately, unlike trench earthquakes, which typically have a shallow fault plane and a steep auxiliary nodal plane.

The high level of present seismicity suggests that the eastern, convergent part of the diffuse boundary is continuing to absorb an increasing amount of shortening. How future shortening will be taken up is unclear. Possibly the diffuse plate boundary will increase in north-south extent. If it extends much farther north it would encounter the Indian continental margin and its great mechanical discontinuity, which might eventually be the site of a trench. Alternatively, further shortening may be taken up over the present extent of the diffuse boundary, which might lead to greater bending and higher stresses and would perhaps further thin the elastic core of the lithosphere. This process might eventually lead to the formation of a throughgoing fault with the potential of becoming a subducting trench if the convergence rate is fast enough. The convergent part of the diffuse boundary, which has already existed for millions of years, may evolve into a discrete plate boundary through this or some other mechanism. However, because little or no thrust faulting occurs where the shortening rate is now fastest, greater shortening west of 86°E may lead not to the formation of a trench but to the predominance of strike-slip faulting.

Extensional Plate Boundary: Diffuse or Discrete?

The western portion of the plate boundary takes up significant north-south extension (~6±2 mm/yr between 10°S, 68°E and 0°S, 68°E) between India and Australia. The distribution of earthquakes and the consistent pattern of tensional axes of most of the focal mechanisms suggests that

the boundary is diffuse, not discrete (Figures 1 and 2). If it is diffuse, its existence disagrees with some widely held views about the differences between discrete extensional boundaries, which occur entirely within oceanic lithosphere, and diffuse extensional boundaries, which are known best from continental examples. Why continental lithosphere extends diffusely and oceanic lithosphere extends discretely is widely attributed to the contrasts in rheology between oceanic and continental lithosphere. The existence of an apparently diffuse India-Australia extensional boundary suggests that the integrated rate of extension across the boundary zone may also affect whether extension is discrete or diffuse. The greatest rate of present extension summed across the East African Rift valleys is ~3 mm/yr [DeMets et al., 1990], the integrated extension across the entire Basin and Range province of western North America is ~10 mm/yr [Clark et al., 1987], and the maximum integrated extension rate across the apparently diffuse India-Australia boundary is ~6 mm/yr. In contrast, the slowest documented present rates of seafloor spreading are total separation rates of ~12 mm/year in the Arctic [Argus et al., 1989] and ~16–18 mm/yr along the Southwest Indian Ridge [DeMets et al., 1988], although Late Cretaceous and early Tertiary spreading between Australia and Antarctica may have been as slow as 9 mm/yr [Cande and Mutter, 1982]. Thus a minimum separation rate may be required for a narrow spreading center to form, although rheology is surely also important.

Weighing against this suggestion is the observed slow extension of oceanic lithosphere within a narrow zone along two present plate boundaries, the Terceira rift and the Dalrymple trough. Magnetic lineations that parallel the narrow Terceira rift near the western end of the Eurasia-Africa plate boundary cannot be convincingly correlated with the reversal time scale [Searle, 1980]. Krause and Watkins [1970], mainly using the width of what they interpret to be the central magnetic anomaly, estimated a separation rate of ~5 mm/yr, which is close to the ~4 mm/yr estimated by Argus et al. [1989] from an analysis of spreading rates, transform azimuths, and earthquake slip vectors in the entire Atlantic. The Dalrymple trough, which connects to the northern end of the Owen fracture zone in the Arabian sea, is also a slowly extending oceanic boundary, which divides the Arabian plate from the Indian plate. Although magnetic anomalies have been recognized, they have not been correlated to the magnetic reversal time scale. From an analysis of plate motion data in the Arabian Sea and Gulf of Aden, Gordon and DeMets [1989] estimated that motion taken up across the Dalrymple trough is only ~2 mm/yr. Neither of these extensional boundaries have morphology resembling typical slowly separating spreading centers; nevertheless they are narrow extensional boundaries. The analogy of the western India-Australia plate boundary to other slowly separating oceanic extensional boundaries suggests the existence of an undiscovered narrow boundary separating the Indian and Australian plates near the Central Indian Ridge. Alternatively, the India-Australia extensional boundary may be wide because of its youth but may later evolve into a narrow boundary. New, detailed bathymetric and magnetic data are needed to discriminate between these possibilities.

Implications for Rigid Plate Models

Many prior studies have argued that the deformation in the equatorial Indian Ocean is midplate or intraplate [Eittreim and Ewing, 1972; Stein and Okal, 1978; Weissel et al., 1980]. These arguments were supported by the work of Minster and Jordan [1978] and Stein and Gordon [1984], who attributed the large, significant nonclosure of the Indian Ocean plate circuit (i.e., through the Indo-Australian, African, and Antarctic plates) to nonrigidity of one or more of these plates, in particular the Indo-Australian plate. In our prior study, when we proposed that India and Australia lie on distinct plates separated by a diffuse plate boundary, we still found significant nonclosure of the Australia-Africa-Antarctica plate circuit and emphasized that the rigid plate model was an idealization [Wiens et al., 1985].

In contrast to these earlier studies we have recently shown that motion about both the India-Arabia-Africa and Africa-Australia-Antarctica plate circuit are consistent with closure, suggesting that the rigid plate idealization is an excellent one [DeMets et al., 1988, Gordon and DeMets, 1989]. In this paper we took the further step of combining these data together to estimate an accurate India-Australia Euler vector. The good agreement between predicted rigid plate velocities and independent observations of the rate and direction of deformation within the diffuse Australia-India plate boundary zone attests to the usefulness and accuracy of the rigid plate model.

Further evidence favoring a model of rigid plates divided by a diffuse plate boundary comes from the rate of plate motion predicted along the boundary. Consider the velocities observed along several zones of lithospheric deformation widely accepted as plate boundaries. Motion along the Owen fracture zone, accepted as a plate boundary since the inception of the plate tectonics model, is only ~2 mm/yr [Gordon and DeMets, 1989]. The East Africa rift, thought by some but not all geologists to be a plate boundary, extends at ~3 mm/yr at its northern end and more slowly to the south [DeMets et al., 1990]. Motion along the Azores-Gibraltar ridge, widely accepted as part of the boundary between the African and Eurasian plates, is only 4 mm/yr, but the Africa-Eurasia velocity may be as high as 7 mm/yr in the eastern Mediterranean near Sicily [Argus et al., 1989]. Motion between the North American and South American plates does not exceed 3 mm/yr [DeMets et al., 1990; D. F. Argus and R. G. Gordon, The present motion and boundary between the North American and South American plates, submitted to *Journal of Geophysical Research*, 1989]. The velocity between Australia and India, 7±4 mm/yr near the Ninetyeast ridge (Table 2), is as fast as or faster than all these, further supporting a model with distinct Australian and Indian plates.

DIRECTIONS FOR FUTURE RESEARCH

The lack of data along the Carlsberg and northern Central Indian Ridge from ~2°N to 12°S makes it hard to locate the India-Australia-Africa triple junction and to test whether it is discrete, diffuse but narrow, or wide. Therefore new accurate magnetic surveys run normal to the ridge segments are

needed, as are surveys of the transform faults using side scan or narrow-beam sonar systems. Marine geophysical data describing the seafloor in the western reaches of the diffuse boundary are sparse. Detailed surveys could test our predictions of north-south extension, show whether the extensional zone is narrow or diffuse, and show how the extension occurs.

When did India-Australia motion start, and how has it evolved? A detailed quantitative chronology is needed to understand how the formation of the diffuse boundary is related to the start of rifting in the Gulf of Aden, the reversal of the Owen fracture zone from left-lateral to right-lateral slip, and the uplift of the Himalayas. Recently, Ocean Drilling Project Leg 116 dated the onset of basement deformation at 7 Ma [Cochran et al., 1987]. A detailed analysis of the history of India-Australia motion would be an important contribution that would quantify the deformation and provide predictions that can be compared with other geological and geophysical data. However, available plate motion data may be too sparse for a convincing model, and new, detailed magnetic surveys over a very large region will probably be needed.

The prediction that the distance between India and Australia is decreasing is testable with space geodetic data. For example, the India-Australia Euler vector predicts that the chord between Calcutta and Sydney is shortening by 12±3 mm/yr, a rate now measurable by both very long baseline interferometry and satellite laser ranging.

It is also important to try to understand precisely how the motion between India and Australia is distributed throughout the diffuse plate boundary. Our rigid plate model places quantitative constraints on integrals of the deformation gradient along surface paths that connect the Indian to the Australian plate. One problem is to understand if the small variation in strike of the basement fold axes is consistent with the nearby location of the Euler vector. The fold axes suggest that the principal direction of shortening is nearly north-south over the entire region of folding. This is clearly not parallel to small circles about the Euler vector and suggests that further study is needed to understand how the structures in the deforming zone are related to the motions of the bounding rigid plates.

CONCLUSIONS

1. Plate motion data record and can be used to estimate the motion between India and Australia.
2. Plate motion data suggest that the Australia-India-Africa triple junction lies between 9°S and 4°N along the Central Indian Ridge, in good agreement with the latitudinal limits of the nearby Chagos seismic zone, but more plate motion data are needed to test and narrow the limits.
3. The plate motion model depends only weakly on whether India and Arabia are treated as one plate or two.
4. The new model gives predictions differing from our prior model [Wiens et al., 1985]: (1) north-south convergence is slower than previously predicted, (2) north-south extension is predicted near Chagos Bank where convergence was previously predicted, and (3) negligible motion is predicted from 75°E to 80°E, a nearly aseismic region where north-south convergence of 8 mm/yr was previously predicted.
5. Predicted velocities of the assumed-rigid plates bounding the deforming zone agree well with observed directions and rates of deformation, supporting the validity and usefulness of the rigid plate model.
6. The rapid north-northwest-south-southeast contraction predicted east of 86°E is hard to reconcile with the observed deformation unless some of the observed strike-slip earthquakes occur not on north-south striking fault planes but on east-west or northeast-southwest striking fault planes, permitting Indian Ocean seafloor to be transported to the northeast where it can be consumed in the Sumatra trench.
7. Our model can be tested further with new plate motion data along the Central Indian Ridge, space geodetic data measuring motion between India and Australia, marine geophysical data from the diffuse plate boundary, and quantitative models of the deformation distributed within the diffuse plate boundary.

Acknowledgments. We thank Doug Wiens and Dave Petroy for results before publication, Alice Gripp for helpful discussions, and Paul Stoddard for help with his map-making program. This work was supported by NSF grants EAR-8721306 and OCE-8900090 and was completed while C. DeMets was an NRC post-doc at the Naval Research Laboratory.

REFERENCES

Argus, D. F., R. G. Gordon, C. DeMets, and S. Stein, Closure of the Africa-Eurasia-North America plate motion circuit and tectonics of the Gloria fault, *J. Geophys. Res., 94,* 5585–5602, 1989.

Bergman, E. A., and S. C. Solomon, Earthquake source mechanisms from body waveform inversion and intraplate tectonics in the northern Indian Ocean, *Phys. Earth Planet. Inter., 40,* 1–23, 1985.

Bergman, E. A., J. L. Nabelek, and S. C. Solomon, An extensive region of off ridge normal-faulting earthquakes in the southern Indian Ocean, *J. Geophys. Res., 89,* 2425–2443, 1984.

Cande, S. C., and J. C. Mutter, A revised identification of the oldest sea-floor spreading anomalies between Australia and Antarctica, *Earth Planet. Sci. Lett., 58,* 151–160, 1982.

Clark, T. A., D. Gordon, W. E. Himwich, C. Ma, A. Mallama, and J. W. Ryan, Determination of relative site motions in the western United States using Mark II very long baseline radio interferometry, *J. Geophys. Res., 92,* 12741–12750, 1987.

Cloetingh, S., and R. Wortel, Regional stress field of the Indian plate, *Geophys. Res. Lett., 12,* 77–80, 1985.

Cochran, J., D. Stow, and Leg 116 shipboard scientific party, Collisions in the Indian Ocean, *Nature, 330,* 519–521, 1987.

DeMets, C., R. G. Gordon, and D. F. Argus, Intraplate deformation and closure of the Australia-Antarctica-Africa

plate circuit, *J. Geophys. Res., 93* 11877–11897, 1988.
DeMets, C., R. G. Gordon, D. F. Argus, and S. Stein, Current plate motions, *Geophys. J. Int.,* in press, 1990.
Dziewonski, A. M., and J. H. Woodhouse, An experiment in systematic study of global seismicity: Centroid-moment tensor solutions for 201 moderate and large earthquakes of 1981, *J. Geophys. Res., 88,* 3247–3271, 1983.
Dziewonski, A. M., J. E. Franzen, and J. H. Woodhouse, Centroid-moment tensor solutions for October–December, 1984., *Phys. Earth Planet. Inter., 39,* 147–156, 1985.
Eittreim, S., and J. Ewing, Mid-plate tectonics in the Indian Ocean, *J. Geophys. Res., 77,* 6413–6421, 1972.
Geller, C. A., J. K. Weissel, and R. N. Anderson, Heat transfer and intraplate deformation in the central Indian Ocean, *J. Geophys. Res., 88,* 1018–1032, 1983.
Gordon, R. G., and C. DeMets, Present-day motion along the Owen fracture zone and Dalrymple trough in the Arabian Sea, *J. Geophys. Res., 94,* 5560–5570, 1989.
Gutenberg, B., and C. F. Richter, *Seismicity of the Earth and Associated Phenomena, 2nd ed.,* Princeton University Press, Princeton, N.J., 1954.
Haxby, W. F., Gravity field of the world's oceans, Map, Natl. Ocean. and Atmos. Admin., Boulder, Colo., 1987.
Krause, D. C., and N. D. Watkins, North Atlantic crustal genesis in the vicinity of the Azores, *Geophys. J. R. Astron. Soc., 19,* 261–283, 1970.
McAdoo, D. C., and D. T. Sandwell, Folding of oceanic lithosphere, *J. Geophys. Res., 90,* 8563–8569, 1985.
McKenzie, D. P., The initiation of trenches: A finite amplitude instability, in *Island Arcs, Deep-Sea Trenches, and Back-Arc Basins, Geophys. Monogr. Ser.,* Maurice Ewing vol 1, edited by M. Talwani and W. C. Pitman, pp. 57–61, AGU, Washington, D.C., 1977.
Minster, J. B., and T. H. Jordan, Present-day plate motions, *J. Geophys. Res., 83,* 5331–5354, 1978.
Molnar, P., and P. Tapponnier, Cenozoic tectonics of Asia: Effects of a continental collision, *Science, 189,* 419–426, 1975.
Petroy, D. E., and D. A. Wiens, Historical seismicity and implications for diffuse plate convergence in the northeast Indian Ocean, *J. Geophys. Res., 94,* 12,301–12,319, 1989.
Schlanger, S. O., and S. A. Stein, Charles Darwin and Captain Moresby on the drowning of the Great Chagos Bank: 19th century discovery of "aseismic" ridge seismicity in the Indian Ocean, *Eos Trans. AGU, 68,* 140–141, 1987.
Searle, R., Tectonic pattern of the Azores spreading centre and triple junction, *Earth Planet. Sci. Lett., 51,* 415–434, 1980.
Spiegel, M. R., *Schaum's Outline of Theory and Problems of Probability and Statistics,* 372 pp., McGraw-Hill, New York, 1975.
Stein, C. A., S. A. P. L. Cloetingh, and M. J. R. Wortel, Seasat-derived gravity constraints on stress and deformation in the northeastern Indian Ocean, *Geophys. Res. Lett., 16,* 823-826, 1989.
Stein, S., An earthquake swarm on the Chagos-Laccadive Ridge and its tectonic implications, *Geophys. J. R. Astron. Soc., 55,* 577–588, 1978.
Stein, S., and R. G. Gordon, Statistical tests of additional plate boundaries from plate motion inversions, *Earth Planet. Sci. Lett., 69,* 401–412, 1984.
Stein, S., and E. A. Okal, Seismicity and tectonics of the Ninetyeast Ridge area: Evidence for internal deformation of the Indian plate, *J. Geophys. Res., 83,* 2233–2245, 1978.
Sykes, L. R., Seismicity of the Indian Ocean and a possible nascent island arc between Ceylon and Australia, *J. Geophys. Res., 75,* 5041–5055, 1970.
Thomas, G. B., Jr., *Calculus and Analytic Geometry,* Addison-Wesley, Reading, Mass., 1972.
Weissel, J. K., R. N. Anderson, and C. A. Geller, Deformation of the Indo-Australian plate, *Nature, 287,* 284–291, 1980.
Wiens, D. A., Historical seismicity near Chagos: A complex deformation zone in the equatorial Indian Ocean, *Earth Planet. Sci. Lett., 76,* 350–360, 1986.
Wiens, D. A., and S. Stein, Age dependence of oceanic intraplate seismicity and implications for lithospheric evolution, *J. Geophys. Res., 88,* 6455–6468, 1983.
Wiens, D. A., and S. Stein, Intraplate seismicity and stresses in young oceanic lithosphere, *J. Geophys. Res., 89,* 11,442–11,464, 1984.
Wiens, D. A., C. DeMets, R. G. Gordon, S. Stein, D. Argus, J. F. Engeln, P. Lundgren, D. Quible, C. Stein, S. Weinstein, and D. F. Woods, A diffuse plate boundary model for Indian Ocean tectonics, *Geophys. Res. Lett., 12,* 429–432, 1985.
Zoback, M. L., and M. D. Zoback, State of stress in the conterminous United States, *J. Geophys. Res., 85,* 6113–6156, 1980.
Zuber, M. T., Compression of oceanic lithosphere: An analysis of intraplate deformation in the Central Indian Basin, *J. Geophys. Res., 92,* 4817–4826, 1987.

D. F. Argus and R. G. Gordon, Department of Geological Sciences, Northwestern University, Evanston, IL 60208.
C. DeMets, Naval Research Laboratory, Code 5110, Washington, D.C. 20375.

(Received March 20, 1989;
revised September 22, 1989;
accepted September 25, 1989.)